Research Article | Vol. 24, No. 26 | 26 Dec 2016 | OPTICS EXPRESS 29349

Optics EXPRESS

Versatile optical laser system for experiments at the European X-ray free-electron laser facility

M. Pergament, G. Palmer, M. Kellert, K. Kruse, J. Wang, L. Wissmann, U. Wegner, M. Emons, D. Kane, G. Priebe, S. Venkatesan, T. Jezynski, F. Pallas, and M. J. Lederer*

European X-Ray Free-Electron Laser-Facility GmbH, Holzkoppel 4, 22869 Schenefeld, Germany
**max.lederer@xfel.eu*

Abstract: We present the main features of the final prototype of a pulsed optical laser, developed for pump-probe and other experiments in conjunction with the femtosecond x-ray beams at the European X-ray free-electron laser facility. Adapted to the temporal x-ray emission pattern of the facility, the laser provides 10 Hz bursts of up to 600 µs duration with intra-burst pulse frequencies as high as 4.5 MHz. In this mode, we have generated pulses as short as 12 fs at 350 W average power during the burst and with beam qualities close to the diffraction limit. This is, to the best of our knowledge, the highest power to date of a few-cycle laser operating at a center wavelength of 800 nm. Important for experimental flexibility, the laser can be configured in various unique ways, enabling, e.g., energy scaling to >3 mJ per pulse through a frequency change down to 100 kHz and the generation of nearly transform limited pulses between 12 fs and 300 fs. In addition to the 800 nm femtosecond beam line, a synchronized long pulse (0.8 ps or 400 ps) 1030 nm beam can be utilized, offering up to 4 kW burst average power, i.e. up to 40 mJ per pulse at 100 kHz. Efficient nonlinear wavelength conversion and tuning through intrinsic and external means further enhance the capabilities of the laser.

©2016 Optical Society of America

OCIS codes: (140.7090) Ultrafast lasers; (190.4970) Parametric oscillators and amplifiers; (190.4410) Nonlinear optics, parametric processes.

References and links

1. "Technical Design Report (TDR) of the European XFEL" (Chapter 6: Photon Beamlines and Scientific Instruments), *http://xfel.desy.de/localfsExplorer_read?currentPath=/afs/desy.de/group/xfel/wof/EPT/TDR/XFEL-TDR-final.pdf*
2. M. Pergament, M. Kellert, K. Kruse, J. Wang, G. Palmer, L. Wissmann, U. Wegner, and M. J. Lederer, "High power burst-mode optical parametric amplifier with arbitrary pulse selection," Opt. Express **22**(18), 22202–22210 (2014).
3. A. Dubietis, G. Jonusauskas, and A. Piskarskas, "Powerful femtosecond pulse generation by chirped and stretched pulse parametric amplification in BBO crystal," Opt. Commun. **88**(4-6), 437–440 (1992).
4. G. Cerullo and S. De Silvestri, "Ultrafast optical parametric amplifiers," Rev. Sci. Instrum. **74**(1), 1 (2003).
5. K. Kruse, M. Pergament, M. Kellert, C. Mendez, G. Kulcsar, and M. J. Lederer, "All-fiber 1030nm burst-mode front-end amplifier for the European XFEL pump-probe laser development for the European X-Ray Free-Electron Laser Facility," Paper Mo4.5, Ultrafast Optics Conference IX, 04–08 March 2013, Davos.
6. P. Russbueldt, T. Mans, G. Rotarius, J. Weitenberg, H. D. Hoffmann, and R. Poprawe, "400W Yb:YAG Innoslab fs-Amplifier," Opt. Express **17**(15), 12230–12245 (2009).
7. M. Kellert, M. Pergament, K. Kruse, J. Wang, G. Palmer, G. Priebe, L. Wissmann, U. Wegner, M. Emons, J. Morgenweg, T. Mans, and M. J. Lederer, "5kW burst-mode femtosecond amplifier system for the European XFEL pump-probe laser development," Talk CA-3.5, (Conference on Lasers and Electro-Optics (CLEO) Europe 2015), 21–25 June 2015, Munich.
8. T. R. Schibli, J. Kim, O. Kuzucu, J. T. Gopinath, S. N. Tandon, G. S. Petrich, L. A. Kolodziejski, J. G. Fujimoto, E. P. Ippen, and F. X. Kaertner, "Attosecond active synchronization of passively mode-locked lasers by balanced cross correlation," Opt. Lett. **28**(11), 947–949 (2003).
9. C. Iaconis and I. A. Walmsley, "Spectral phase interferometry for direct electric-field reconstruction of ultrashort optical pulses," Opt. Lett. **23**(10), 792–794 (1998).

#276302 http://dx.doi.org/10.1364/OE.24.029349
Journal © 2016 Received 21 Sep 2016; revised 25 Oct 2016; accepted 29 Oct 2016; published 12 Dec 2016

Optics EXPRESS

10. SNLO nonlinear optics code available from A. V. Smith, AS-Photonics, Albuquerque, NM *http://www.as-photonics.com/snlo*
11. T. Lang, A. Harth, J. Matyschok, T. Binhammer, M. Schultze, and U. Morgner, "Impact of temporal, spatial and cascaded effects on the pulse formation in ultra-broadband parametric amplifiers," Opt. Express **21**(1), 949–959 (2013).
12. S. Adachi, T. Horio, and T. Suzuki, "Generation of intense single-order harmonic pulse in the vacuum ultraviolet region using a deep ultraviolet driving laser," Opt. Lett. **37**(11), 2118–2120 (2012).
13. TOPAS-prime, http://www.lightcon.com/Product/TOPAS-Prime.html

1. Introduction

User operation at the six experimental stations of the European X-ray Free-Electron Laser Facility (XFEL) necessitates a dedicated, synchronized optical pump-probe (PP-laser). The requirements specification for such a laser can be condensed from the science cases of the facility's experimental stations ("scientific instruments") on the one hand, and the peculiarities of the XFEL emission on the other [1]. The former typically leads to relatively standard specs such as ultrashort pulse durations ranging from a few optical cycles to several 100 fs, pulse energies of a few µJ to mJ, as well as different wavelengths - all depending on the science. The XFEL emission, however, is quite specific, owing to the burst-mode operation of the accelerator: up to 27000 x-ray femtosecond pulses per second are emitted in 10 Hz bursts of 600 µs duration and with up to 2700 pulses per burst, i. e. up to 4.5 MHz within the bursts. Meeting all requirements in combination is clearly outside the scope of today's off-the-shelf laser technology, hence the need for development.

In an earlier report we presented both the concept and intermediate experimental results from the PP-laser prototype [2]. We had achieved burst average powers of more than 30W and single pulse energies up to 180 µJ from the 800 nm signal-wave of a 2-stage BBO non-collinear optical parametric amplifier (NOPA) [3,4], pumped by the second harmonic of a 1030 nm, 400 W picosecond laser amplifier. Other features included sub-15 fs pulse duration, arbitrary (single) pulse selection, nearly diffraction limited beam quality and 100 nm wavelength tuning directly from the NOPA.

In the current work we scaled both the burst average power and single pulse energy of the prototype by more than one order of magnitude. We also show the capability of producing pulses between <15 fs and 300 fs duration, which are close to the transform limit. Finally, wavelength conversion and tuning are demonstrated using conversion stages and a collinear parametric amplifier, pumped by the PP-laser NOPA. With these results, the PP-laser development for the European XFEL has been concluded successfully. The installation of three systems will commence in fall 2016.

2. Experimental setup

The concept of the PP-laser prototype was introduced in some detail in [2]. Here, we are showing it in Fig. 1 with emphasis placed on major upgrades since. An all-fiber chirped pulse front-end amplifier (CPA), which is operated in 10 Hz burst-mode with 5% duty cycle, provides two inherently synchronized outputs [5]. It is seeded by a 54 MHz, 1030 nm femtosecond oscillator (Origami-10) with low intrinsic jitter (<7 fs rms), synchronized to an RF-reference. Later, the XFEL synchronization will employ both RF- and optical links for residual jitter values below 20 fs rms. One output of the front-end amplifier is compressed to 300 fs and then used to generate 7 nJ of white light continuum (WLC) pulses in a YAG-crystal, which seed the first of up to three sequential NOPA stages. The intra-burst frequency of the seed path is fixed at 4.5 MHz, whilst an acousto-optic modulator (AOM) allows arbitrary selection of seed pulses. WLC have proven to be a stable and reliable seed source for ultra-short pulse parametric amplifiers, assuring excellent beam quality and compressibility. In this context, dispersion management plays an important role in the conception of our NOPA. Using different magnitudes of pre-chirp on the WLC, short as well as longer pulses can be created through temporal filtering by the pump pulse, whereby the compressed pulses

Optics EXPRESS

are almost transform limited. For the shortest pulses, our dispersion management uses chirped mirrors with a dispersion which is conjugate to that of fused silica. A relatively small amount of pre-chirp suffices to amplify the maximum allowable spectrum for good quality pulse re-compression, as dictated by the dispersion bandwidth of the mirrors (ca. 180 nm). After amplification and suitable adaptation of beam size, bulk fused silica is used as a compressor (short pulse mode). Typically, we have a "fused silica budget" of up to 50 mm in this mode. For longer pulses, a considerably higher magnitude of pre-chirp is required. Here, pre-chirp dispersion is reversed, conveniently combining material and mirrors to result in the conjugation of a compact unfolded Treacy compressor in transmission (long pulse mode) [2]. As for the limitations of this scheme, we find the shortest pulse duration to be limited by our current design of chirped mirrors, which allow values somewhat below 15 fs. With increasing chirp, the long pulse limit was experimentally located around 300 fs, where efficient amplification in the first stage starts to degrade due to a lack of seed photon spectral density for the 800 fs pump pulses.

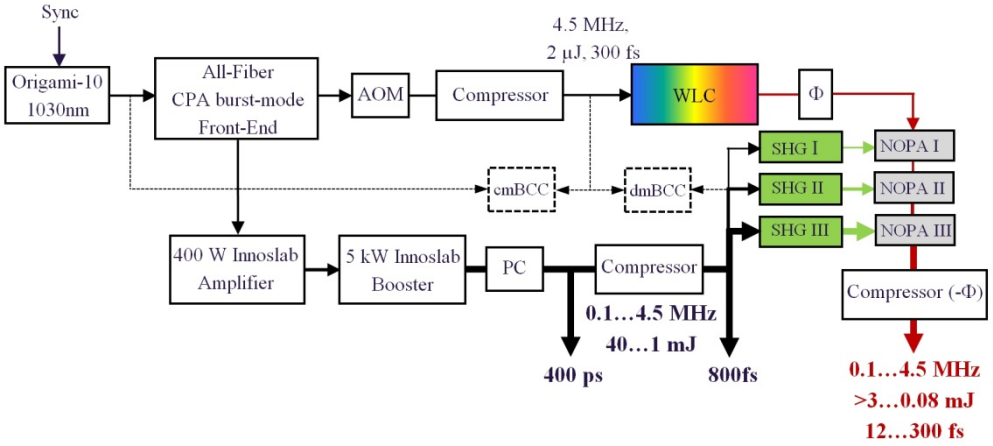

Fig. 1. Schematic of the PP-laser prototype: AOM (Acousto-Optical Modulator), PC (Pockels cell), SHG (Second Harmonic Generation), Φ (dispersion management with multi-bounce chirped mirrors and/or material), cmBCC (common mode Balanced Cross Correlator), dmBCC (differential mode Balanced Cross Correlator), NOPA (Non-collinear Optical Parametric Amplifier). Seed and pump beams are controlled by beam pointing stabilization systems.

The other front-end output provides variable repetition rate, 1.3 ns long chirped pulses to seed a 400 W Innoslab Yb:YAG pre amplifier [6], followed by a 5 kW Innoslab booster amplifier [7]. The pre and booster amplifiers are quasi-cw pumped, i. e. work in 10 Hz burst-mode with burst durations of 2.5 ms and 1.3 ms respectively. They reach full saturation during the burst, which means that a change of intra-burst repetition rate from 4.5 MHz to 100 kHz (as set in the front-end) ensues a change in single pulse energy from 1.1 mJ to 50 mJ at the output. To achieve the necessary beam quality (M^2<1.25) for second harmonic generation and NOPA pumping, the booster beam is spatially filtered. This, and some further losses incurred in the reflective multi-layer dielectric grating compressor (grating size: 300mm x 80mm) and delivery optics, leads to an available burst power of 4 kW, corresponding to 40 mJ at 100 kHz and 800 fs pulse duration. The latter is limited by the gain bandwidth of the Yb:YAG Innoslab amplifier, which results in an amplified spectral width of around 2 nm. A Pockels cell (PC) and polarizer were inserted before the compressor, enabling the picking of arbitrary pump pulse sequences from the amplified burst at frequencies up to 4.5 MHz.

The compressed infrared pulses are split into beam replicas of suitable intensity for frequency doubling and subsequent pumping of the NOPA stages. Four NOPA configurations were tested, corresponding to the actual set points of the PP-laser (see Table 1). All four

Optics EXPRESS

configurations provide output pulses with comparable compressibility and beam quality. The NOPA pulse energies, reached during experiments, are also listed in Table 1.

Even small temperature and humidity changes can cause pulse timing drifts both between the XFEL and the PP-laser (common-mode), as well as between the pump and seed pulses on the laser table (differential-mode). To compensate for these, balanced cross-correlators (BCCs) [8] are used in feed-back loops. Similar sensitivities to environmental changes are observed regarding beam pointing, which are taken care of by active pointing stabilization for both the seed and pump beams of the NOPA. As mentioned above, the PP-laser beam delivery consists of two beam lines, one for the 800 nm NOPA output and the other for the 1030 nm uncompressed or compressed pulses from the amplifier chain. It is even conceivable to operate both beam lines simultaneously, for instance, if NOPA I + II were operated at around 300 µJ (nominally set point 2) at 100 kHz, instead of 1.13 MHz. Appropriate means for power redistribution are implemented. In the following section we mainly concentrate on the results from the NOPA and its conversion.

Table 1. Operating set points of the PP-laser

Set point	Rep-rate (MHz)	NOPA	E_{NOPA} (mJ)
1	4.5	I + II	0.08
2	1.13	I + II	0.325
3	0.188	I + II + III	1.8
4	0.1	I + II + III	3.25

3. Results

3.1 NOPA pump conditions

Operating parametric amplifiers at vastly different pump energies can be difficult. To make use of the maximum pump energy dynamics of 1:40, enabled by our front-end and pump amplifiers, we have chosen a NOPA design with three stages and four set points (see Table 1). In the interest of facility up-time, the setup time when switching between set points should be as short as possible, i.e. the required changes simple and minimal. Therefore, the following guide lines were applied in the design:

- Spot sizes on SHG and NOPA crystals of respective stages are fixed and do not change with set points
- Fluences (SHG and NOPA) for NOPA I are the same for all set points
- Set point changes 1 ⇨ 2 and 3 ⇨ 4 require different crystal thicknesses in stages II and III respectively.
- The beam paths for all set points are identical, i.e. the beams of set points 1 and 2 propagate through NOPA III, which is not pumped in this case.

Following these principles, we can reset the NOPA in the worst case merely by changing thin crystals and making power and timing adjustments on the pump beams to optimize performance, but without re-imaging and re-routing.

Determining suitable fluences on SHG and NOPA crystals, as well as their lengths, is usually guided by maximization of conversion efficiency. However, fluences which are too high can trigger undesirable effects (self-focusing, filamentation, damage), whilst highly saturated nonlinear amplification tends to degrade beam quality. Similarly, we found in previous work [2], that the pump beam quality is crucial for good beam quality of amplified beams. In our experiments we have previously used both Beta-Bariumborate (BBO) and Lithium Triborate (LBO) crystals for SHG and NOPA, which, after length optimization, rendered virtually identical results and were found to have no discernible influence on beam quality and efficiency. Nevertheless, BBO is preferred for the NOPA due to practical reasons (larger non-collinearity angle).

Optics EXPRESS

Figure 2 shows the near field profiles of the actual pump beams (after SHG) of the three NOPA stages. The intensities (crystal lengths) are for NOPA I: 35 GW/cm^2 (2.5 mm), NOPA II: 9 – 34 GW/cm^2 (2 mm and 1.5 mm), NOPA III: 32 – 60 GW/cm^2 (1.3 mm and 1.1 mm).

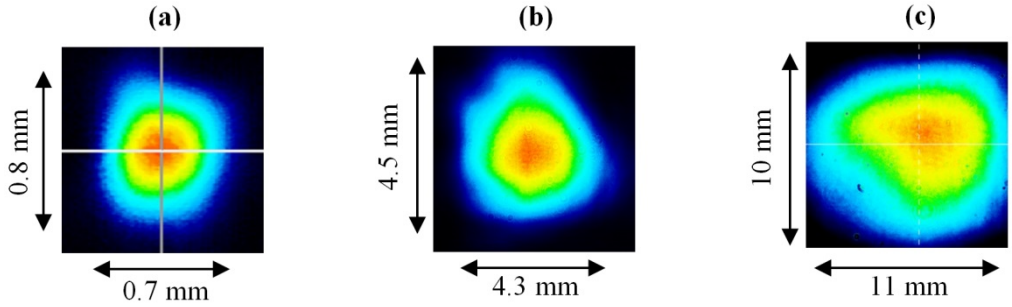

Fig. 2. Near field profiles of the NOPA pump beams (515 nm). (a) NOPA I, (b) NOPA II, (c) NOPA III. The given dimensions are 1/e^2 diameters from Gaussian intensity fits. Ellipticity and Gaussian intensity fit values are >90% in all cases. The images were taken with an exposure time of 80 µs near the center of a single burst.

3.2 NOPA characteristics

The output spectra of all four set points are shown in Fig. 3. The green curves in both graphs represent the output spectrum of NOPA I in the case of the "short-pulse" dispersion scheme. As mentioned above, the first stage is operating under the same pumping conditions (35 GW/cm2) for all set points, providing 8 µJ of seed energy with differing spectral bandwidth according to the chosen dispersion management. The red and blue curves in Fig. 3(a) demonstrate the second stage output spectra at 4.5 MHz and 1.1 MHz with corresponding output energies of 80 uJ and 325 uJ. The average power during the burst is therefore more than 350 W. The output spectra of the three-stage amplifier are shown in Fig. 3(b) with red and blue curves depicting the 188 kHz and 100 kHz set points respectively. With output energies of 1.8 mJ and 3.25 mJ, the burst average power exceeds 300 W in these cases. Spectral narrowing due to multi-stage amplification are not observed and the spectra are virtually identical from 80 µJ to >3 mJ. The near field beam profiles depicted in the insets of Fig. 3 attest to the beam quality obtained from both amplifier configurations.

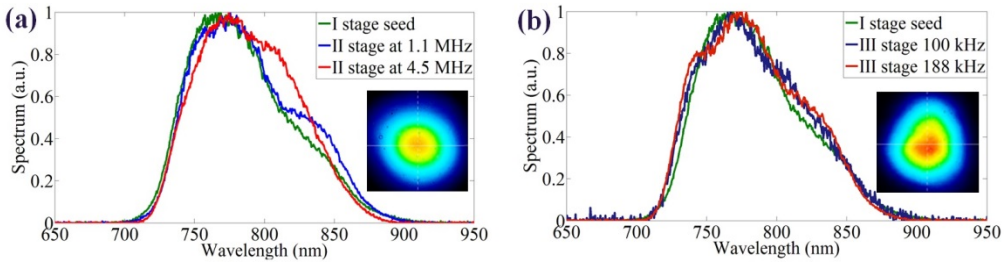

Fig. 3. Spectral characteristics of multistage amplifier in short pulse mode. (a) two stages (set points 1 and 2), (b) three stages (set points 3 and 4). Insets show images of the near field beam at the output. Spectra and images were taken with an exposure time of 80 µs near the center of a single burst.

The beam quality of a NOPA is determined by the level of saturation, but also by the seed and pump beam quality. As for the seed source, WLC have an almost perfectly diffraction limited beam quality (see also [2]). The quality of the pump is especially important in multi-stage amplifiers, where it has to be good for every stage (confirm Fig. 2). Examples of caustic scans of the NOPA with two and three stages are presented in Figs. 4 and 5 respectively. For

Optics EXPRESS

two stages in particular, beam shapes render a Gaussian Intensity fit quality >94% over more than 15 Rayleigh ranges. An estimation of the M^2 results in a value smaller than 1.1.

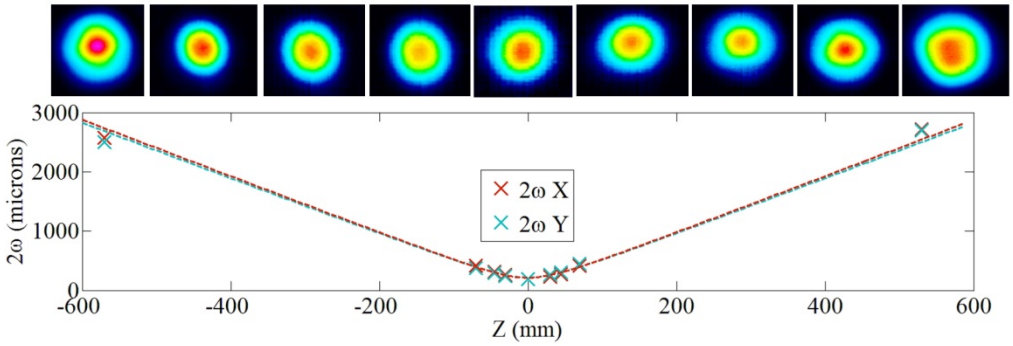

Fig. 4. Caustic scan of the two stage NOPA: 1.13 MHz rep-rate, 350 µJ single pulse energy. The Gaussian intensity profile fit quality is >94% over 15 Rayleigh ranges. Data points with crosses correspond to the beam images, taken with an exposure time of 40 µsec at the center of a single burst. The dashed lines depict the fitted caustic, used to estimate an M^2<1.1.

For three stages we observe a slight degradation of beam quality along with minor astigmatism. According to our understanding, this can be explained by the different spatial amplification profile in the vertical and horizontal planes, caused by the asymmetry of the third stage pump beam [see also Figs. 2(c) and 3(b)]. Nevertheless, the beam can be fit with Gaussian intensity profiles with a fit quality of >92% over more than 5 Rayleigh ranges. The estimated M^2 is smaller than 1.2.

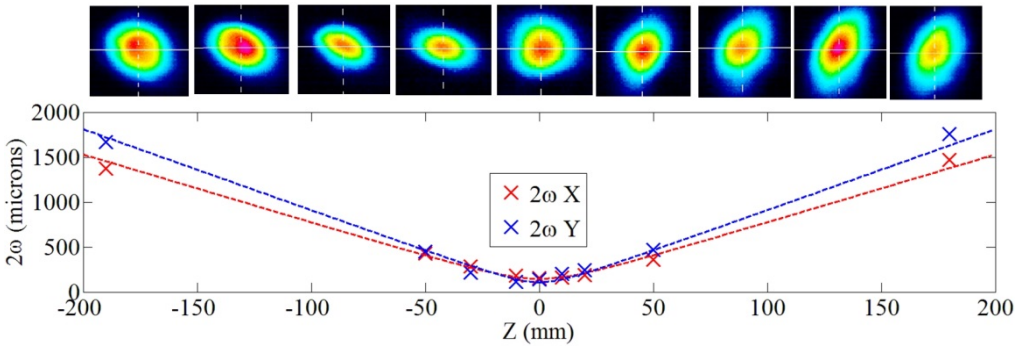

Fig. 5. Caustic of three stage NOPA: 100kHz rep-rate, 3.25mJ single pulse energy. Gaussian intensity profile fit >92% over 5 Rayleigh ranges. Data points with crosses correspond to the beam images, taken with an exposure time of 40 µsec at the center of a single burst. The dashed lines depict the fitted caustic, used to estimate an M^2<1.2.

As was described earlier, by varying the magnitude of the pre-chirp on the WLC, we can generate nearly transform limited pulses from <15 fs to 300 fs. The required spectral filtering happens mainly in the first stage of amplification, where the 800 fs pump pulse cuts the corresponding spectrum for the targeted pulse duration from the WLC. Figure 6 shows the temporal and spectral characterization of two extreme cases. The NOPA is operating in set point 4, i.e. with three stages, at a 100 kHz rep-rate and with a pulse energy of 3.25 mJ. For the short pulse mode, the blue curves depict the temporal intensity of a sub-15 fs pulse [Fig. 6(a)] as reconstructed by the SPIDER method [9] and the corresponding spectrum [Fig. 6(b)]. To this limit, the dispersive mirror pair matches the dispersion of the fused silica compressor rather well, as is witnessed by the high pulse contrast and flat spectral phase (confirm [2]). With even less pre-chirp and some degradation of the contrast, sub-12 fs compressed pulses are possible. Switching to long pulse mode, we find a practical limit at pulse durations around

Optics EXPRESS

300 fs, above which effective amplification in the first stage starts to degrade due to a lack of seed photon spectral density. The red curves show the autocorrelation [Fig. 6(a)] and spectrum [Fig. 6(b)] for this case. Note, that at this limit, pulse compression becomes unnecessary. The autocorrelation was measured without compressor.

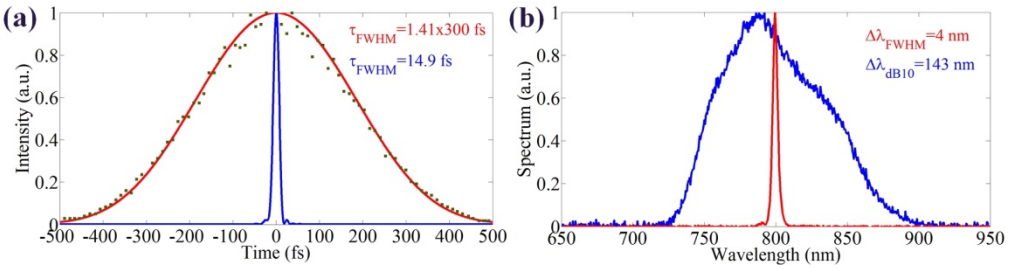

Fig. 6. Characterization of amplified pulses at 100 kHz intra-burst rep-rate, 3.25 mJ single pulse energy. (a) blue curve, short pulse mode: reconstructed pulse shape using SPIDER and red curve, long pulse mode: autocorrelation, (b) corresponding spectra, taken with an exposure time of 80 µs near the center of a single burst.

The fact that the different pulse durations can be configured while remaining close to the transform limit, enables applications requiring broadband short pulse excitation or spectral selectivity and efficient conversion and tuning, all using the same laser source. This is unique and ultimately enabled through the simple means of dispersion management, which is possible with the sub-ps pumped NOPA scheme, employed in the PP-laser.

In earlier work, we showed the capability of generating arbitrary NOPA pulse sequences down to single pulse selection using either the AOM in the seed generation path or the Pockels cell (PC) in the pump path [2]. The resulting NOPA bursts were flat and showed no dependence on the total amount of energy within the burst. Since then, we have added a burst-mode booster amplifier to scale the pump power by one order of magnitude. The total burst energy to the SHG crystals of the last NOPA stages is now 2.5 J. It is therefore interesting to reexamine the temporal burst behavior both intra-burst and burst-to-burst to see if thermal effects from linear or nonlinear absorption in the SHG and NOPA crystals are still negligible. In Figs. 7(a) and 7(b) we compare photodiode traces of two extreme situations (set point 4). One shows the complete 600 µs long burst, the other only two pulses, generated at around the middle of the burst. The pump energy therefore differs by a factor of 30. There is evidence of pulse energy variation across the 600 µs burst, which originates in the intra-burst energy and beam size dynamics of the booster amplifier, while pulse to pulse noise in the burst is <1% rms, hence quite low.

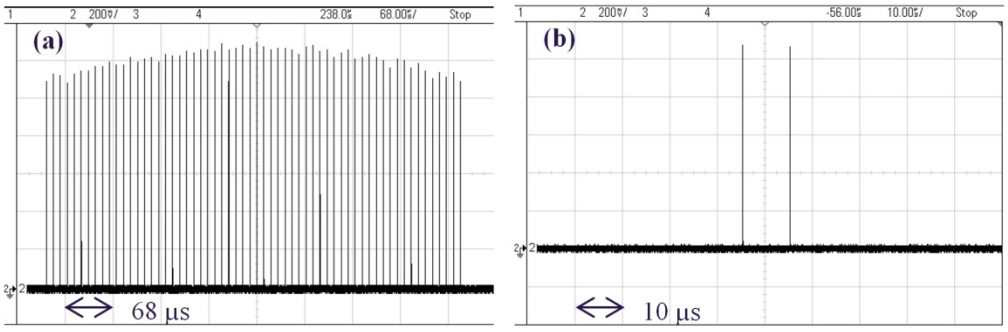

Fig. 7. Different modes of burst operation at 100 kHz intra-burst rep-rate (set point 4). (a) full 600 µs long burst, (b) two selected pulses. The PC was used for burst and pump pulse selection.

Optics EXPRESS

In Fig. 8 we analyze the two burst cases in terms of near field beam profile and spectral evolution through the burst. For this, we performed scanning measurements with 200 µs delay steps. The camera and spectrometer both had an exposure time of 80 µs, capturing 8 pulses at 100 kHz. The slight pulse energy variation through the burst, seen in Fig. 7(a), is also observed in the beam intensity, whilst the spectra look steady. Comparing these beam shapes and spectra with those from only two pulses we conclude, that there is no substantial thermal effect induced through linear or nonlinear absorption either in the SHG or NOPA crystals in the burst-mode operation.

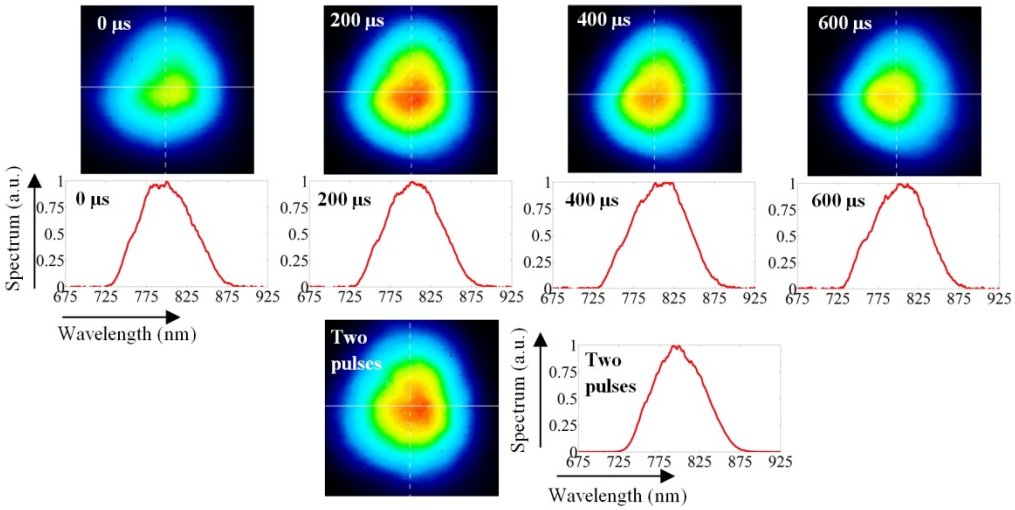

Fig. 8. Intra-burst scanning measurement of near field profile and spectra. (top) full 600 µs long burst (200 µs steps), (bottom) two pulses only. Spectra and images are of a single burst and were taken with an exposure time of 80 µs.

While intra-burst pulse to pulse energy stability is currently limited by the aforementioned dynamics in the prototype booster amplifier, burst to burst stability is largely dominated by air fluctuations. The prototype system has a stability of around 2% rms, which we expect to improve through suitable coverage, as planned for future systems.

3.3 Frequency conversion

Since many experiments at the European XFEL will rely on selective optical excitation processes, wavelength tunability of the PP-laser will be a key feature for scientific users. In earlier work, we explored the tuning range obtainable from the NOPA directly. Obviously, tuning comes at a loss of pulse bandwidth. Nevertheless, at 50 fs, the NOPA could be tuned over a range greater than 100 nm with little loss of pulse energy [2]. Providing tunable fs-pulses to users will to some extent rely on this feature, combined with second (SHG) and third harmonic generation (THG). In addition, to extend capabilities further, we will also utilize the NOPA pulses to pump a commercial optical-parametric-amplifier system. In this section we present the results of these efforts.

BBO was chosen for all SHG and THG experiments. All of the crystals were cut for type I critical phase matching. Some crystals (thickness <110 µm and clear aperture >22 mm) could only be procured glued to a 1 mm thick fused silica carrier-substrate. Prior to the measurements, conversion simulations with both the SNLO [10] and Chi2D [11] software packages were performed to estimate optimum crystal properties. The NOPA was operated at set point 4 (100 kHz) for highest output energy and was then consecutively set to two different dispersion points for two different pulse durations. With the short pulse setting and a 50 mm bulk fused silica compressor, 15 fs pulses where generated. The beam diameter was set to 20 mm ($1/e^2$) to keep the B-integral low through the compressor. The 1mm carrier-

Optics EXPRESS

substrate of the SHG-BBO crystals served as the final compression segment in the path of the 800 nm beam. Both SHG and THG were done with a beam diameter of 8 mm. The pulse energy was varied by a broad-band attenuator before the compressor. The maximum pulse energy on the SHG crystal was somewhat compromised by losses in the attenuator and peaked 2.4 mJ, where the peak intensity was 670 GW/cm^2.

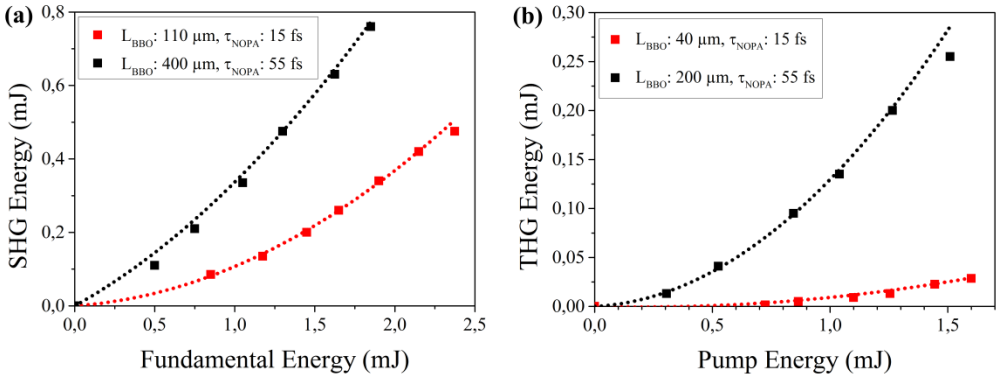

Fig. 9. Measured pulse energies for SHG (a) and for THG (b) at 15 fs (red) and 55 fs (black) pulse duration, dotted curves show results from simulations with Chi2D.

SHG conversion simulations suggest optimum crystal lengths of 90 – 110 µm, where the group velocity mismatch limits further lengthening. At 110 µm length, we achieved the highest SHG energy of 475 µJ at a maximum conversion efficiency of η_{SHG} = 20%. The measured energy curve and power spectrum are plotted in Figs. 9(a) and 10(a), respectively. As soon as the peak intensity of the pump exceeds 600 GW/cm^2, the accumulated B-integral reaches about 2 rad, which reduces beam quality. Despite the high intensities, no damage was observed.

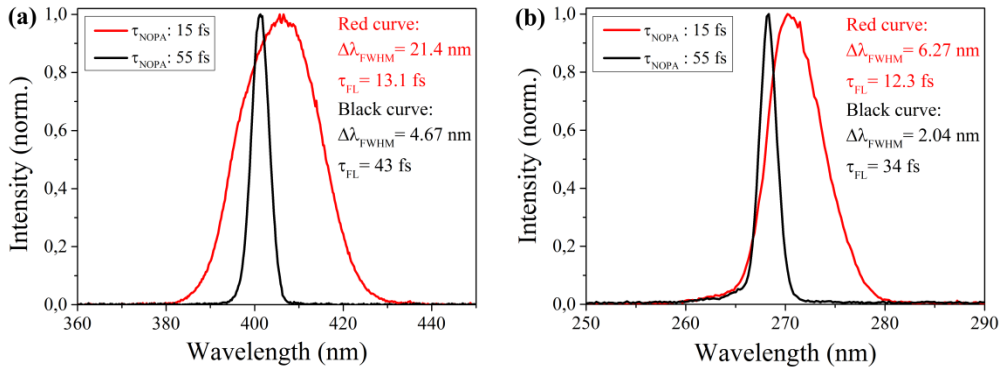

Fig. 10. Measured power spectra for SHG (a) and THG (b) at 15 fs (red) and 55 fs (black) pulse duration, τ_{FL}: theoretical pulse duration limit from Fourier transformation estimating flat phase with no dispersion contribution.

THG simulations suggest that group velocity mismatch restricts the maximum crystal length to less than 50 µm, which was utilized in the following tests. After SHG, the fundamental beam was temporally delayed and it propagated through one separating and one combining mirror. The polarization of the 400 nm pulse was rotated behind the first separator to meet type I phase matching criteria in the collinear THG-stage together with the 800 nm pulse. Before the conversion process, both wavelengths propagate through the 1 mm fused silica carrier of the BBO-crystal. As a consequence, both pulses are chirped which limits the available conversion efficiency and pulse energy. The highest measured pulse energy was 28 µJ. This comes at an overall conversion efficiency of η_{THG} = 1.7%. To match these results in

Optics EXPRESS

simulation, the 800 nm pulses had to be chirped to between 60 and 90 fs. In the future we intend to improve conversion efficiency to 3 – 5% by reducing the amount of dispersion in the fundamental beam path. Furthermore, there is a more elegant all-in-line configuration for THG, involving thin (≈100µm) delay compensator and wave plates. It enables substantially higher conversion efficieny (>10%) at the shortest pulse durations [12] and will be the method of choice, once carrier-free crystal plates with our target clear aperture of 22mm or larger become technologically viable.

The NOPA dispersion was then reconfigured for the long pulse mode and to amplify the spectral bandwidth of a 55 fs pulse. As described in section 2, compression is accomplished in this mode by a compact Treacy transmission grating compressor. The additional losses incurred in the compressor currently limit pulse energies to 1.75 mJ. Using the same beam diameter and collimation as previously and longer BBO-crystals, SHG and THG were evaluated for the new pulse parameters. The highest SHG energy of 760 µJ was now generated with a 400 µm long BBO-crystal, corresponding to a conversion efficiency of 43%. Figure 9(a) shows the measured and simulated conversion curves, whereas Fig. 10(a) depicts the corresponding SHG power spectrum. In the case of THG, 100 µm and 200 µm long BBO crystals were used. With the 200 µm long crystal, pulse energies of 255 µJ were achieved at 17% conversion efficiency. In contrast to the 15 fs case, dispersion had negligible impact on the pulse duration in this case. Figures 9(b) and 10(b) show the conversion measurements with simulation and THG spectrum for this case respectively. After hours of operation we still achieved the same UV-energy, although, onset of typical UV-radiation induced degradation of the BBO rear coating could be observed.

For all conversion experiments we investigated the presence of absorption (e. g. two-photon-absorption) within 100 – 600 µs burst length. Such effects could be caused by caloric heating during the burst, leading to changes of phase-matching and conversion efficiency. Neither a change of intra-burst energy distribution nor burst-to-burst effects, attributable to heat accumulation, were observed.

Finally, to extend the wavelength range even further, we have tested a commercial optical-parametric amplifier (OPA), covering the majority of the spectrum between 250 nm and 15 µm as shown in Fig. 11. The TOPAS-prime series [13] is usually pumped by Ti:Sapphire amplifier systems with repetition rates in the lower kHz range and millijoule energies. Therefore it was the first time that the TOPAS-prime was pumped with a NOPA that provides mJ pulse energies in burst-mode.

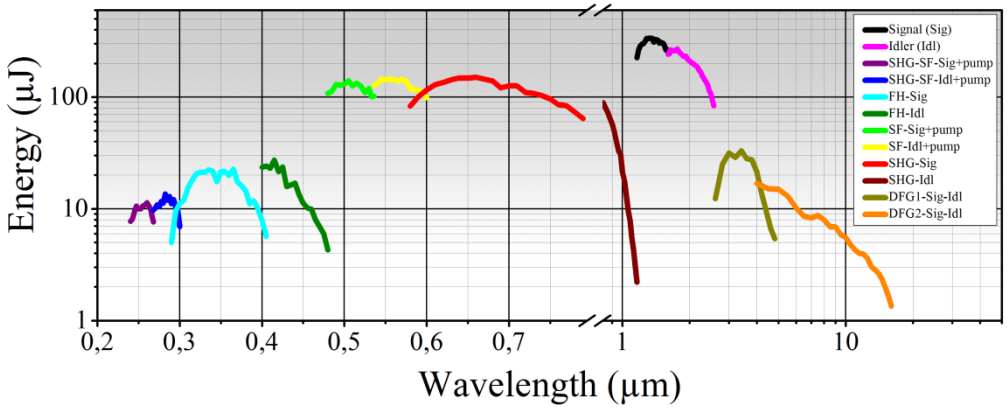

Fig. 11. Tuning curves of TOPAS-prime with VIS and IR extensions when pumped by the 55 fs, 1.75 mJ, 100 kHz burst-mode pulses from the PP-laser.

The utilized unit consisted of a TOPAS-prime (with fresh-pump option), a UV-VIS-extension and a long-wavelength IR extension (NDFG). The device was pumped with a pulse

Optics EXPRESS

energy of 1.75 mJ at a pulse duration of 55 fs. Like in previous measurements the pump beam diameter was 8 mm ($1/e^2$). The experiments showed that the TOPAS device works well with the NOPA pump source and results, similar to those using standard pump sources were achieved. No evidence of heat accumulation could be detected on any time scale.

4. Summary

We presented the main features of the final prototype of a femtosecond laser, developed for pump-probe and other experiments in conjunction with the femtosecond x-ray beams at the European XFEL. The laser concept is based on sub-ps pumped multi-stage NOPAs, and offers unique performance, matching the 10 Hz burst-mode operation of the facility. With experimental flexibility in mind, the pump-probe laser is configurable in 4 set points, corresponding to intra-burst repetition rates between 4.5 MHz and 100 kHz with single pulse energies ranging from 80 µJ to 3.25 mJ, respectively. Other features include burst average powers >350 W at a center wavelength of 800 nm, near transform limited pulses from 12 fs to 300 fs, near diffraction limited beam quality, single pulse selection up to 4.5 MHz and the possibility to utilize a second synchronized beam line with up to 40 mJ, 800 fs or 400 ps, 1030 nm pulses, corresponding to a burst power of 4 kW. Finally, we showed the efficacy of the pump-probe laser in wavelength conversion and tuning, using both harmonic generation and a commercial optical parametric amplifier. During the development, major efforts were directed also towards fail safe long term operation and the monitoring and control integration of the laser into the facility control system. With these results, experimental work has been concluded successfully. Following design finalization, installation of 3 systems will commence in fall 2016.

131.169.135.91 {ts '2017-01-09 08:55:19'}